Stereoblock Polypropylene/Isotactic Polypropylene Blends. III. Isothermal Crystallization Kinetics of iPP Component

S. CANEVAROLO and F. DE CANDIA*

Dipartimento di Ingegneria Chimica e Alimentare, Universitá di Salerno, 84081 Fisciano, Salerno, Italy

SYNOPSIS

The isothermal crystallization of blends of stereoblock polypropylene and isotactic polypropylene were analyzed. The main interest in this phenomenon is related to the steric affinity between the two components. The composition of the blend was changed over a wide range. The obtained results demonstrate the incompatibility of the two components both in the liquid phase and the solid state. © 1995 John Wiley & Sons, Inc.

INTRODUCTION

The blends based on isotactic polypropylene (iPP) are widely studied for their many applications. Probably the most studied systems are the PP/ethylene–propylene random copolymers.[1] In the present article we report about a bicomponent system based on iPP and a stereoblock PP. The feature of the stereoblock system is a particular steric order characterized by short isotactic sequences with continuously changing absolute configuration.[2] The stereoblock polymer shows properties described in previous studies,[3,4] and its blends with the iPP, obtained by rapid cooling from the melt, have been recently described.[5,6] The samples at lower content of isotactic iPP showed good elastic properties, both in terms of deformation reversibility and energy dissipation in the hysteresis cycles, and it was suggested a model based on the presence of a physical network, in which the crosslinking is due to cocrystallization between the matrix (the stereoblock PP) and the crystalline domains of iPP.[5,6] We consider the isothermal crystallization, and particularly its kinetic aspects.

EXPERIMENTAL

Materials

The materials employed in this work were the stereoblock PP (sbiPP) previously used[2] and the iPP RAPRA (Great Britain). The blends were obtained by dissolving the two components in hot xylene and then casting a film at 80°C. The solvent casting was followed by compression molding at 190°C in a Carver hot press, and the molten films were rapidly quenched to 0°C in an ice-water bath.

Samples were prepared in a wide composition range starting from pure iPP up to a blend containing 5% iPP. Each sample is herein identified by the iPP content in weight percent, i.e., 90 iPP is a sample containing 90% in weight of iPP and 10% of sbiPP.

The crystallization of the iPP component was measured by differential scanning calorimetry (DSC) using a Mettler TA 3000 DSC purged with nitrogen and chilled with liquid nitrogen. All samples were subjected to a standard thermal cycling: a fast heating up to 200°C, an isothermic treatment at this temperature for 2 min, a fast cooling (at 30°C/min) to the required crystallization temperature (90°C $\leqq T_c \leqq$ 130°C), an isothermic treatment long enough to allow a complete crystallization of the iPP component, and finally a heating scan from 30 to 200°C at 30°C/min. To minimize the effects of the thermal lag in the sample during the crystallization, each data curve was processed by subtracting the data curve of a pure sbiPP sample subjected to the same thermal cycling, i.e., acting as baseline; sbiPP was chosen because it has almost the same thermal properties as the iPP and does not crystallizes in this temperature range. With this procedure almost all curves assume a straight baseline, but in the few cases in which this was not possible, a polynomial curve was fitted. During the measurements of the

* To whom correspondence should be addressed.

Journal of Applied Polymer Science, Vol. 57, 533–538 (1995)
 CCC 0021-8995/95/050533-06

melting enthalpy of the iPP component, the minimum temperature limit was the same temperature at which the sample was crystallized.

RESULTS

To follow the isothermal crystallization of the iPP phase during the cooling from the melt, the DSC thermograms of sbiPP/iPP blends were analyzed first in terms of the half-time of crystallization parameter ($t_{1/2}$). Figure 1 shows this parameter as a function of the crystallization temperature for the blends with various iPP contents. Starting from the pure iPP curve, which is quasilinear in the range 110–125°C, the blending with increasing amounts of sbiPP strongly affects the overall iPP crystallization rate. Initially there is a great increase, reaching a maximum effect with 10% sbiPP (sample 90iPP); and then, with a further increase of sbiPP, the overall iPP crystallization rate continuously decreases for further dilution of the iPP component.

The isothermal iPP crystallization kinetics was also analyzed according to the Avrami procedure, i.e., the crystallization conversion parameter, ln $(-\ln(1 - X_{ti}))$, as a function of the crystallization time, $\ln(t)$ in minute, at the various crystallization temperatures. Figure 2 shows some of the Avrami plots of sbiPP/iPP blends. The 50% conversion levels (for $X_{ti} = 0.5$ the $\ln(-\ln(1 - X_{ti})) = -0.366$) and, for each curve, the best fitting slopes within the possible theoretical Avrami exponents (n = 1, 2, 3, or 4) are drawn as guidelines in this graph.

The curves in general are not linear comporting more than one slope, whose values tend to reduce for higher conversions and lower crystallization temperatures. The pure iPP (not shown) shows its data curve fitted well with an Avrami exponent of $n = 3$, reflecting an overall crystallization rate due to the spherulitic growth from nuclei instantaneously formed.

On increasing the sbiPP content, two effects are shown: first, the overall iPP crystallization rate reaches a maximum with sbiPP contents up to 10% and then continuously decreases, as already seen for the $t_{1/2}$ parameter. Moreover there is an increase in the curvature of the plots, which induces a broadening of the possible Avrami exponent. In only few cases, for instance the blend with 50% sbiPP at a crystallization temperature of 130°C, the crystallization kinetics follow closely, in all its crystallization range, the Avrami equation, but, in this case, for an exponent $n = 4$. For blends with a high level of dilution, i.e., 10% or less iPP content, the crystallization kinetics again follow very closely the Avrami theory for an exponent $n = 3$, as in pure iPP.

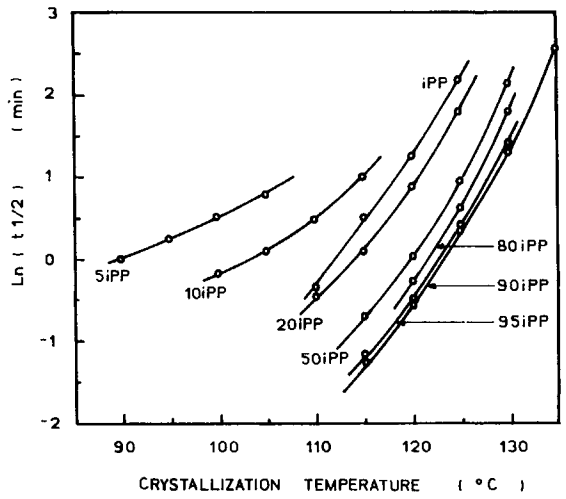

Figure 1 iPP crystallization half-time vs. crystallization temperature for sbiPP/iPP blends with various iPP contents.

We attempted to show graphically this second effect by mapping the Avrami exponent, in the beginning of the crystallization process and toward its final stages. Initially the data curves can be fitted with slopes of n = 3, 4, or even higher. Their values are mapped in Figure 3. These values decrease by the end of the crystallization process, and they can be seen mapped in Figure 4.

Figure 4 shows the boundary lines for the Avrami exponent presented at the end of the crystallization process. These lines are mainly linear, parallel to each other, and nearly horizontal i.e., showing a strong dependence on the crystallization temperature and a weak dependence on the sbiPP content. Conditions inducing high overall crystallization rates are low crystallization temperatures and low sbiPP content; in this case, at the end of the process, the Avrami exponent is $n = 1$, characteristic of a secondary crystallization (a rodlike growth from instantaneous formed nuclei). This value is continuously increased up to $n = 4$ by increasing the crystallization temperature or greatly diluting the iPP chains in the sbiPP component. A large content of sbiPP chains induces a similar effect in the iPP crystallization kinetics as an increase in the crystallization temperature.

Figure 5 shows the constant Z (obtained graphically by extrapolating the Avrami slope curve for $n = 3$ at $\ln t = 0$) as a function of the iPP content for the various crystallization temperatures. This value is that observed for the conversion after 1 min of crystallization, considering an Avrami crystalliza-

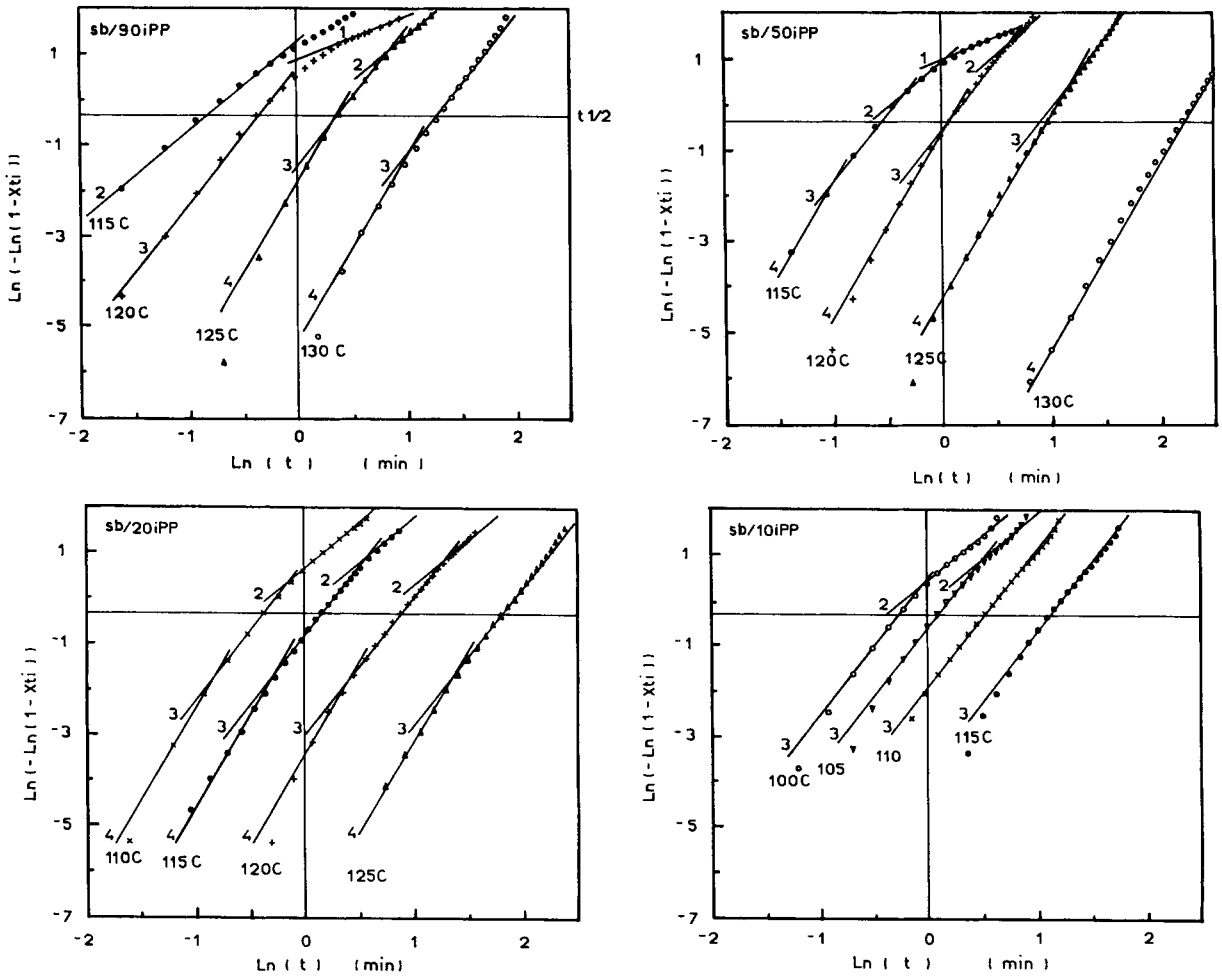

Figure 2 Avrami plots of the iPP crystallization in the sbiPP/iPP blends with various iPP contents and crystallization temperatures.

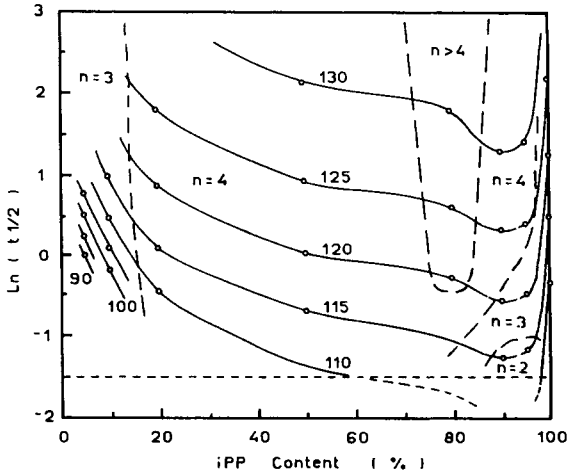

Figure 3 iPP crystallization half-time vs. iPP content for sbiPP/iPP blends at various crystallization temperatures, presenting the boundary lines for the Avrami exponents shown in the beginning of the crystallization process.

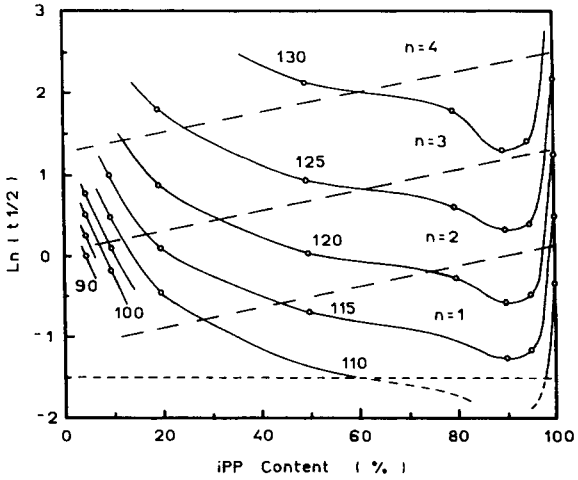

Figure 4 Same as Figure 3, but presenting the boundary lines for the Avrami exponents shown in the final stages of the iPP crystallization process.

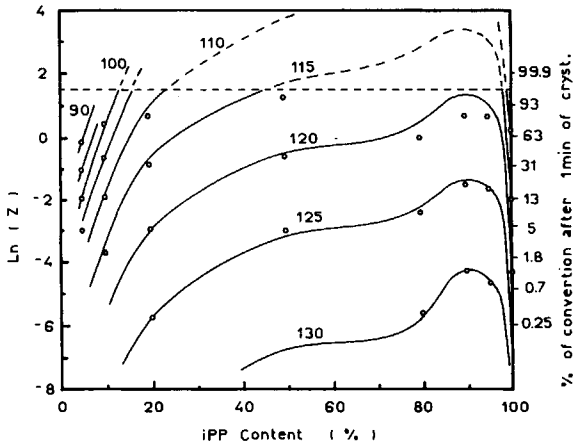

Figure 5 The Z rate constant for the crystallization of the iPP in the sbiPP/iPP blends. The points were obtained graphically and the curves were calculated according to eq. (1).

tion kinetics with $n = 3$. For comparison purposes in this figure, the best fitting curves of the Z rate constant calculated using the Avrami relation with $n = 3$ are also drawn:

$$Z = (t_{1/2}) \times \ln(2). \qquad (1)$$

The experimental data agree well with the calculated curves except when the $\ln(Z)$ values are greater than 1, i.e., for very high levels of conversion (by definition after just 1 min of crystallization). These high levels of crystallization rates not only induce a kinetics with low n values (see Fig. 4), far from the Avrami theory, but also show a greater level of error because they are near to the practical limit of our experimental measurements (shown as a broken line).

The crystallized samples were subjected to a DSC heating scan (at 30°C/min) in order to get some information on the formed crystals, based on their melting behavior. The presence of the sbiPP in the system induces, during the isotherm crystallization at temperatures of $105°C \leqq T_c \leqq 125°C$ and iPP contents from 20 to 80%, the formation of another crystalline phase which, during the following heating, melts at lower temperatures, seen as a shoulder of the melting peak of the iPP phase. Figure 6 shows the thermograms of 20iPP crystallized at various temperatures.

The melt temperature and melting enthalpy of the iPP phase are shown in Figures 7 and 8. Samples with very low or very high iPP contents crystallize with an iPP crystalline content in the range of 52–60%, normalized to the actual content and using $H_o = 165$ J/g which is in the same range of pure iPP.[7] On the other hand samples with intermediate iPP contents ($20\% \leqq$ iPP $\leqq 80\%$) show a much lower value of crystallinity, in the range of 40–45%. The integration of the melting curve was set starting at the crystallization temperature. This particular setting excludes the contribution of any other crystallized phase.

DISCUSSION

On the basis of the obtained results, one can suggest the presence of few main effects ruling the isothermal crystallization process. The first is the influence of sbiPP on the nucleation of the iPP crystallization: this influence seems to be dominant at high contents of PP. The second is the role of sbiPP on the diffusion of the PP chains from the molten mass to the growing crystals. This role is composition dependent, because it is expected to induce a higher diffusion rate at low sbiPP contents, for the reduced viscosity of the molten mass; but as soon as this content increases, the dilution of the iPP becomes an increasing barrier for the growing of the crystals. The trend of the parameter $t_{1/2}$ reflects the first two effects, and indeed this parameter goes through a minimum in sample 10iPP, well below the pure iPP, to continuously increase on decreasing the iPP content. Perfectly symmetric is the trend of the parameter Z of the Avrami equation, which goes through a maximum in sample 10iPP. The temperature effects are not considered in this discussion, because the ruling parameter is the composition, and at any composition the crystallization rate simply increases as the temperature decreases.

Considering now the Avrami analysis, regarding the meaning of the parameter n, it is well known that it contains information including the growing dimensionality, and the nucleation mechanism.[8] For $n = 1$ and $n = 4$ the meaning is unique; for $n = 2$ or 3, and for each of them, there are two possibilities, as known.[8] Moreover on the basis of the n value, some rough hypotheses on the sample morphology can be drawn.

To analyze the obtained results, one can start from the pure iPP, in this case $n = 3$, which in the presence of a spherulitic morphology means instantaneous nucleation. This value is observed in the primary crystallization for high iPP contents, and appears again at very low iPP concentrations. This is a crucial point because it indicates that the crystallization mechanism of iPP is the same at high and low iPP content. An obvious consideration is that the iPP is not compatible with the

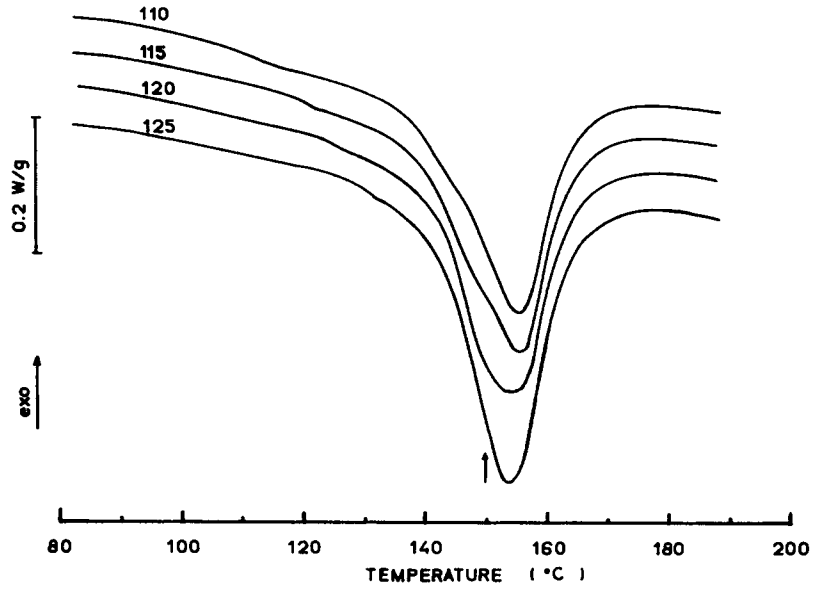

Figure 6 DSC heating thermograms (in the iPP melting range) of sample 20iPP crystallized at various temperatures.

sbiPP. In fact the only possible interpretation is that the fluid mass, in which the crystallization process is activated, contains liquid domains of pure iPP. This allows the exclusion cocrystallization phenomena in isothermal conditions, at temperatures well above the melting of the sbiPP phase. The cocrystallization was indeed observed in very different crystallization conditions, under rapid cooling and under flow.[5,6]

Considering now the intermediate compositions, n assumes prevalently the value 4, which means three-dimensional growth and a time dependent nucleation. This datum, if considered observing the melting behavior that is discussed in the following, indicates a different "structural organization" of the molten mass, where the segregation between the two liquid domains is expected to be finer than in the blend at high and low iPP content, also as an effect of the inversion of the liquid matrices expected at intermediate compositions.

The secondary crystallization in the entire composition range will be not considered, because it is less meaningful for the understanding of the crystallization process.

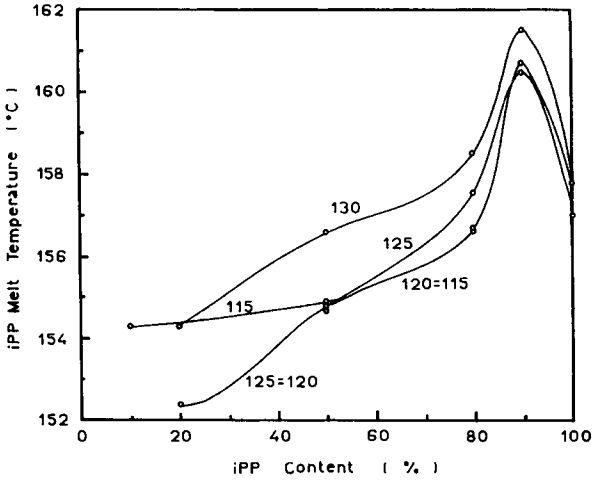

Figure 7 iPP melting temperature as a function of the iPP content in sbiPP/iPP blends, isothermally crystallized at various temperatures.

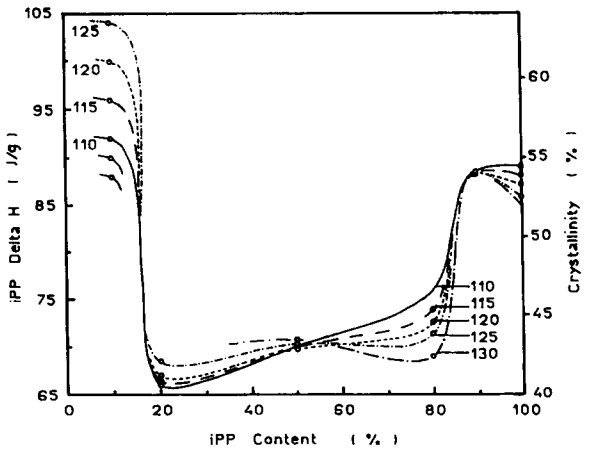

Figure 8 Melting enthalpy of the iPP phase of sbiPP/iPP blends for various iPP contents and crystallization temperatures.

Perfectly in agreement with the crystallization mechanism is the melting behavior where the deep depression of the melting enthalpy and temperature at intermediate compositions indicate thinner and more defective crystals. Moreover the depression of the melting enthalpy means lower crystallinity, which in all the intermediate compositions is lower than in the extreme compositions. It is interesting to note that the crystallinity, normalized to the iPP content, at low iPP content assumes the same values observed in the pure iPP. This effect is further evidence of the total incompatibility of the two components also in the liquid phase, so that the crystallization all occurs inside the well-segregated liquid domains.

One of the authors (S.C.) sincerely acknowledges the financial support given by FAPESP (Research Founding Institution, Brazil).

REFERENCES

1. J. A. Manson and J. H. Sperling, Polymers Blends and Composites, Plenum, New York, 1976.
2. J. A. Ewen, *J. Am. Chem. Soc.*, **106,** 6355 (1984).
3. F. de Candia, R. Russo, and V. Vittoria, *Makromol. Chem.*, **189,** 815 (1988).
4. F. de Candia and R. Russo, *Thermochim. Acta,* **177,** 221 (1991).
5. S. Canevarolo and F. de Candia, *J. Appl. Polym. Sci.,* to appear.
6. S. Canevarolo, F. de Candia, and R. Russo, *J. Appl. Polym. Sci.,* to appear.
7. J. Grebowich, J. F. Lau, and B. Wunderlich, *J. Polym. Sci. Polym. Symp.*, **71,** 19 (1984).
8. R. J. Young and P. A. Lovell, *Introduction to Polymers,* Chapman & Hall, New York 1991.

Received September 6, 1994
Accepted February 7, 1995